J Solid State Electrochem (2007) 11:639–646
DOI 10.1007/s10008-006-0216-x

ORIGINAL PAPER

Catalytic effect of Pd nanoparticles on electroless copper deposition

Chien-Liang Lee · Yu-Ching Huang · Li-Chen Kuo

Received: 30 June 2006 / Revised: 15 August 2006 / Accepted: 20 August 2006 / Published online: 11 October 2006

Abstract This study elucidates the application of Pd nanoparticles as catalysts of electroless copper deposition and their catalytic effect on the deposition kinetics and microstructure in an electroless copper bath. Quartz crystal microgravimetry (QCM) and high-resolution field emission scanning electron microscopy (FE-SEM) with energy dispersive X-ray spectroscopy (EDX) demonstrated that the kinetic changes associated with electroless copper deposition (ECD) comprised two stages—the incubation period and the acceleration period. In the incubation period, small copper particles were deposited. In the acceleration period, the ECD rate increased rapidly and continuously conducting films with large grains were formed. Leaner sweep voltammetry (LSV) and mixed potential theory (MPT) were applied to examine the catalytic powers of the prepared Pd nanoparticles and the related electrochemical kinetics in the ECD bath.

Keywords Nanoparticle · Palladium · Electroless copper deposition · Kinetics · Electroless nickel deposition · Surface modification · Activator

Introduction

Electroless copper deposition (ECD) is an important technology in advanced nanocircuit industries, and is used for printing circuit board (PCB) [1, 2] and manufacturing semiconductors [3–5]. In PCB manufacturing, ECD is commonly performed to deposit conductive copper on the inside wall of the insulating hole of the substrate to connect the electronic components [2]. Similarly, ECD is also an attractive procedure for depositing copper to form interconnections that are smaller than 45 nm in ultralarge-scale integration (ULSI) [6], because it can replace the electrodeposition process, which depends on a preplated copper seed layer formed by an expensive vapor-phase method. Although various factors, such as the composition of the deposition solution [7–9] and the choice of ligands [10, 11], affect the performance of an electroless process, the activation is a key determinant of the rate and mechanism of electroless deposition [12]. Activation, which is a catalytic reaction, is triggered with active colloids on the surface of the substrates dipped in an electroless deposition bath. Meanwhile, the active catalyst is a role as an electron carrier that supports the transfer of electrons from the reducer to the metal ions. Therefore, colloids can be regarded as means of controlling the width and thickness of the lines and the time required for the advanced fabrication of nanocircuits.

ECD is an electrochemical reaction, comprising simultaneous anodic and cathodic reactions, at a particular interface between the electrolyte and the plated substrate. Mixed potential theory (MPT), which yields two Tafel curves of the anodic and cathodic reactions, is frequently adopted to analyze the kinetics of electroless deposition [13, 14]. The points of intersection between the anodic and cathodic Tafel curves yield the deposition current and the mixed potential associated with a deposition reaction in the steady state. Furthermore, quartz crystal microgravimetry (QCM) is a novel method for analyzing in situ the observed electrochemical kinetics based on the change in frequency of the vibration at the electrode [15].

Recently, we synthesized Pd nanoparticles by self-regulated reduction and tested their activities toward an

C.-L. Lee (✉) · Y.-C. Huang · L.-C. Kuo
Material and Chemical Research Laboratories,
Industrial Technology Research Institute,
Rm. 733 Bldg. 52, 195 Sec. 4, Chung Hsing Rd,
Chutung, Hsinchu, Taiwan 310, Republic of China
e-mail: cl_lee@url.com.tw

Table 1 The composition of electroless copper deposition for analyses of linear sweep voltammetry (LSV), mixed potential theory (MPT), and quartz crystal microbalance (QCM)

Composition of electroless copper bath					
QCM		LSV and MPT			
		Oxidation reaction		Reduction reaction	
$CuSO_4$	0.05 mol/dm^3	HCOH	0.27 mol/dm^3	$CuSO_4$	0.05 mol/dm^3
HCOH	0.27 mol/dm^3	EDTA	0.1 mol/dm^3	EDTA	0.27 mol/dm^3
EDTA	0.1 mol/dm^3	pH (adjustment with NaOH)	12.3	pH (adjustment with NaOH)	12.3
pH (adjustment with NaOH)	12.3				

electroless copper and nickel bath [15]. This study further explores the electrochemical effectiveness of the activated Pd nanoparticles in catalyzing ECD. MPT and QCM are applied in cases of various quantities of Pd nanoparticles to compare theoretical and actual ECD kinetics. The ECD deposition rates of these Pd nanoparticles can thus be fairly compared. Furthermore, the microstructure deposited over different deposition times is measured for comparison with the results of high-resolution field emission scanning electron microscopy (FE-SEM). The elemental copper and Pd contents in the deposition layer are analyzed.

Experimental

Preparation of Pd nanoparticles

Palladium nanoparticles were prepared by the following procedure [16]. First, 0.54 g $Pd(OAc)_2$ (palladium acetate) was slowly dissolved in 50 ml of 0.1 M neutral aqueous solution of sodium *n*-dodecyl sulfate (SDS). The hydrophobic group of the SDS micelle then captured the Pd $(OAc)_2$ molecule. The solution was then heated slowly in an oil bath (130 °C) with a reflux system. The initially yellow solution slowly became dark brown and the pH declined from 5~4 to 1, as the reaction proceeded over approximately 7 h. The basic reaction involves the release of alcohol by partial decomposition of the surfactant [16], enabling the reduction of palladium ions. The size, appearance, and crystallinity of the Pd nanoparticles were determined by high-resolution transmission electron microscopy (HR-TEM; JEOL JEM-2000EX).

Analysis of deposition kinetics and microstructure

The synthesized Pd nanoparticles were used an activator to activate ECD. Pd nanocolloids were precipitated by ultrahigh speed centrifugation at 12,000 rpm and redispersed using deionized water, to reduce the influence of SDS on ECD. Table 1 presents the compositions of the ECD bath used to measure the polarization curve and the quartz crystal microbalance (QCM, SEIKO QCA922), respectively. All electrochemical experiments of ECD were

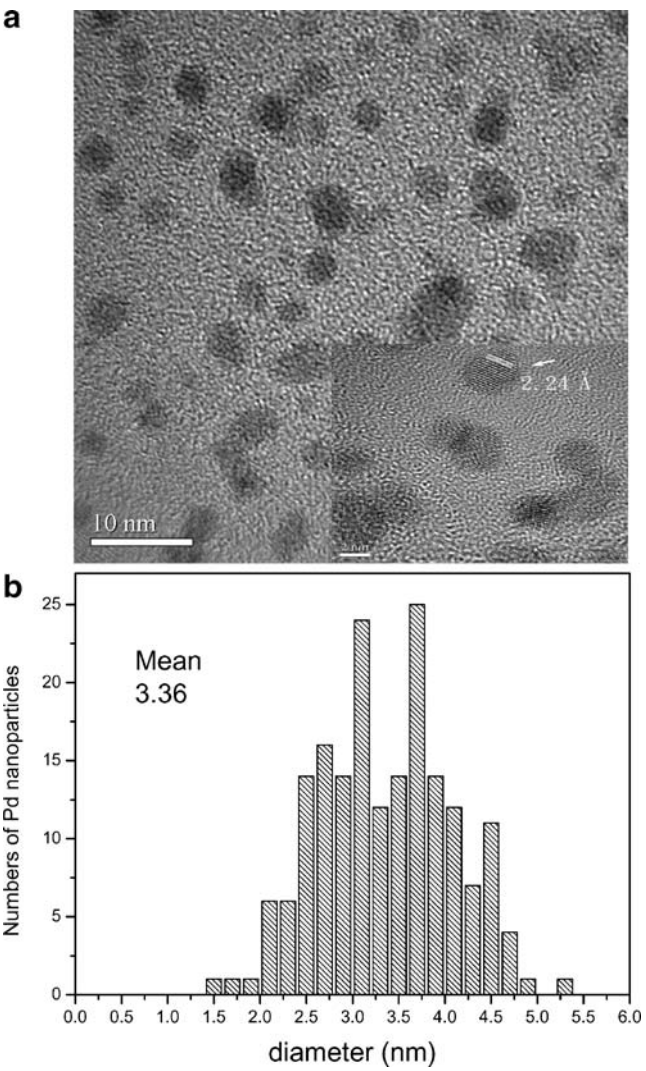

Fig. 1 HR-TEM image of prepared Pd nanoparticles. **a** High-resolution image; **b** calculated size distribution

performed in the baths maintained at 30 °C, through which was bubbled N_2 gas for 15 min before measurements were made.

In linear sweep voltammetry (LSV) and polarization curve analysis, the resulting aqueous solutions were uniformly dropped onto a 0.07 cm^2 glassy carbon electrode (GCE) and heated at 70 °C to evaporate off the water for 5 min. The glass carbon electrode was rinsed by 3 μl 5wt% Nafion solution and heated at 70 °C for 10 min to prevent the catalyst from falling off the electrode. Polarization was measured using a potentiostat (Autolab PGATAT30), incorporating a rotation disk electrode (RDE). A three-electrode cell, comprising a GCE working electrode, a Pt counter electrode, and an Hg/Hg_2Cl_2 reference electrode, was used to make the measurement. The experiment was conducted in anodic or cathodic reaction (Table 1) at a scan rate of 5 mV/s and a rotation speed of the working electrode of 3,600 rpm.

As in the QCM experiment, the working electrode used in the measurement was prepared by applying 2, 3, 4, and 5 μl of Pd nanoparticle solution uniformly on a 0.159 cm^2 Au surface of the QCM substrate. The QCM substrate

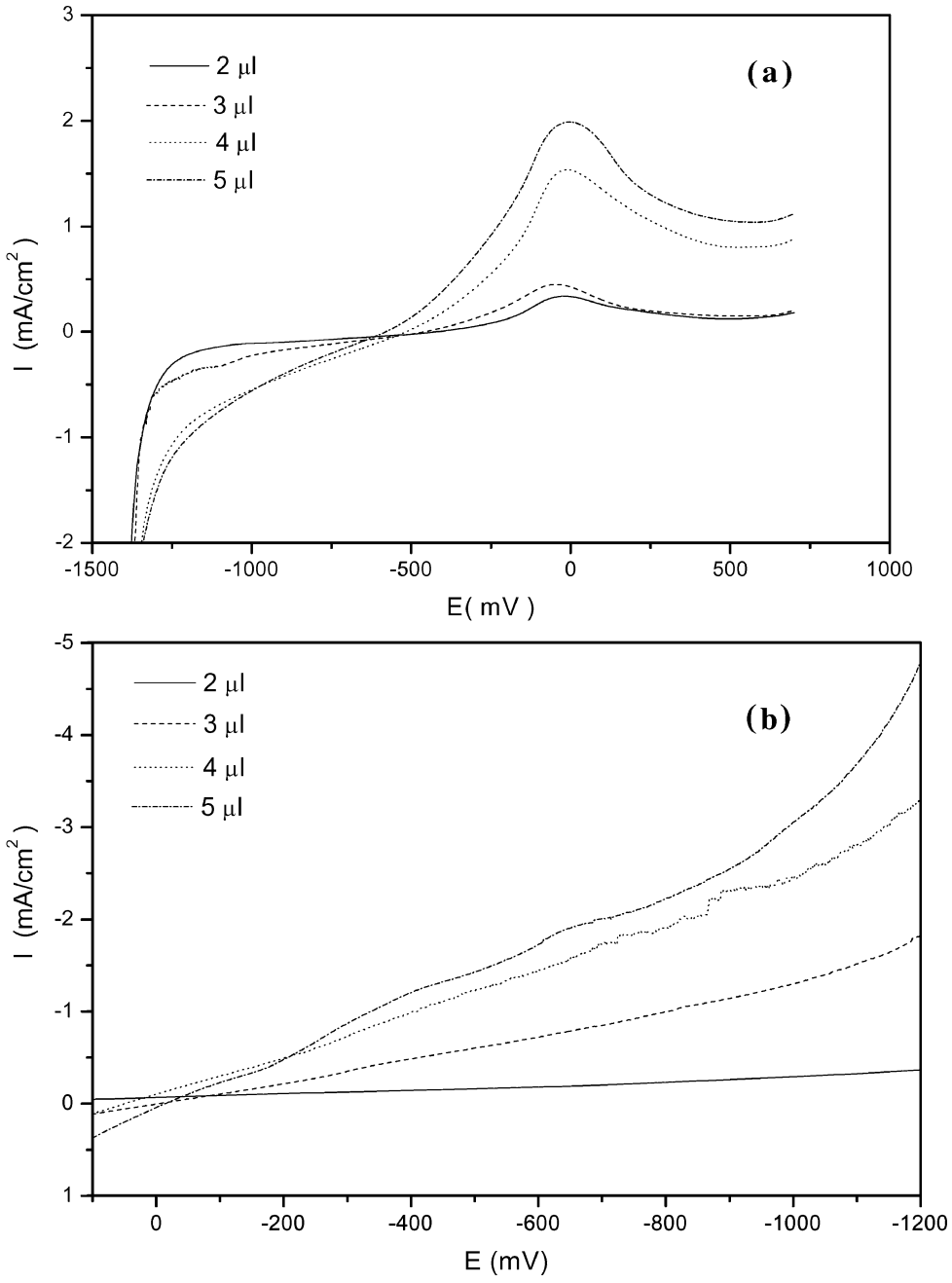

Fig. 2 LSV curves of electroless copper bath catalyzed by increasing amount of Pd nanoparticles in the absence of either formaldehyde or Cu^{2+}. **a** Anodic curve; **b** cathodic curve

(SEIKO EG&G QA20-A9M-Au) was sputtered with gold on a 100 Å titanium film from both sides and was connected to a home-build oscillator. The reference electrode (Hg/Hg_2Cl_2) was separated from the main solution compartment by a Luggin capillary, which was filled with saturated KCl solution.

Various volumes of Pd nanoparticles are dropped into the O ring with a confined area of 0.159 cm^2 and naturally dried on the clear silicon substrate. The activated substrates are dipped into the ECD bath. After the ECD reaction proceeds, the deposited substrates are taken out. The microstructural and elemental analyses are performed by high-resolution field emission scanning electron microscopy (FE-SEM) and energy dispersive X-ray spectroscopy (EDX) (Hitachi S-4700I).

Results and discussion

Figure 1a clearly presents HR-TEM images of prepared Pd nanoparticles used as catalysts of ECD. Pd nanoparticles were synthesized with a narrow size distribution. The lattice spacing was around 2.24 Å, which value is regarded as the lattice space between the [111] planes of metallic palladium [17]. The image analysis by HR-TEM demonstrates that the mean particle diameter was around 3.36 nm, as presented in Fig. 1b.

The oxidative and reductive power of appropriate amounts of Pd nanoparticles for ECD was analyzed by linear sweep voltammetry (LSV). Figure 2 plots the current–potential (I–E) curves for the oxidation of formaldehyde in the anodic bath and the reduction of copper ions in the cathodic bath, whose compositions are presented in Table 1. In the anodic bath, the oxidation reaction was observed at a starting potential of ~−500 mV, as shown in Fig. 2a. The oxidation current density increased slowly with the potential, reaching a diffusion limited current of ~−40 mV. The oxidation current density of the reducer in the ECD bath increases with the number of Pd nanoparticles, indicating that the oxidation power depends on the amount of catalyst in the ECD bath. The reduction reaction at the electrode surface, distributing Pd nanoparticles, occurs at ~−20 mV and the current increased linearly with the potential from ~−20 to ~−1,200 mV, as presented in Fig. 2b. The catalytic power of the reduction current of the copper ions increased with the amount of nanocatalyst. The result was similar to that of oxidation, revealing that not only the oxidative power but also the reductive power in the ECD bath depends on the amounts of catalyst on the electrode surface. Theoretically, in electroless metal deposition, the catalytic particles act as carriers in the transfer of electrons from the reducing agent to the metal ions. The solid catalysts thus importantly affect the kinetics. MPT, which is described by the Tafel equation, is commonly utilized to analyze the rate of electroless metal deposition. According to MPT, the coordinates of the point of intersection between the anodic and cathodic curves yield the deposition current (I_{MPT}) and the mixed potential (E_{MPT}) at which the deposition reaction is in a steady state. Figure 3 plots the electrochemical current–potential curves of the Tafel equation of ECD, catalyzed by various amounts of Pd nanoparticles. The deposition potential and deposition current density, catalyzed by 2 μl of Pd nanoparticles, were ~−210 mV and ~0.112 mA/cm^2, respectively. Notably, a negative shift of E_{MPT} from ~−210 to ~−280 mV occurred as the amount of Pd nanoparticles increased, indicating that an increase in the number of active colloids promote the spontaneous deposition reaction. Then, a small increase in the deposition current density from approximately 0.112 to ~0.796 mA/cm^2 was followed by an increase in the amount of Pd nanoparticles on the electrode surface. The ECD deposition rate (R_{MPT}) obtained by mixed potential theory is given by Faraday's law [18].

$$R_{MPT} = 1.18 \times I_{MPT}$$

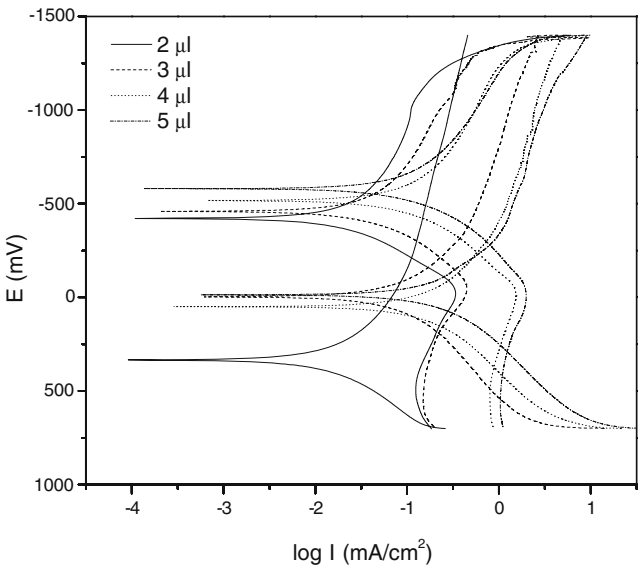

Fig. 3 Anodic and cathodic polarization curves of increasing amounts of Pd nanoparticles as activators of electroless copper deposition

Table 2 The summary for ECD kinetics measured by MPT and QCM

Deposition kinetics	2 μl	3 μl	4 μl	5 μl
E_{MPT} (mV)	−210	−212	−242	−281
I_{MPT} (mA/cm^2)	0.112	0.23	0.576	0.796
Deposition rate (μg/cm^2 s)				
R_{MPT}	0.037	0.075	0.189	0.261
R_{QCM}	0.189	0.282	0.294	0.480
Ratio of R_{QCM} to R_{MPT}	5.1	3.76	1.55	1.83

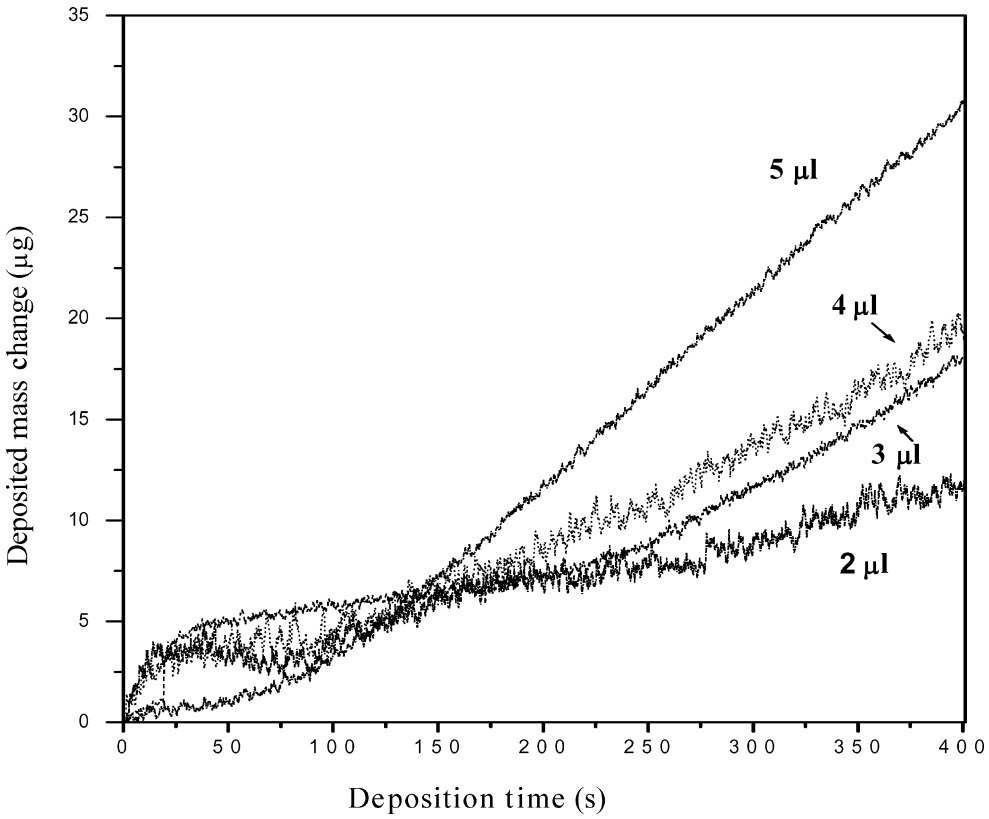

Fig. 4 QCM analyses of the deposition kinetics of electroless copper deposition catalyzed by various amounts of Pd nanoparticles

Table 2 presents the calculated results. The deposition rates of 2, 3, and 4 μl Pd nanoparticles were recalculated to be around 0.037, ~0.075, and ~0.189 μg/cm^2 s, respectively, the R_{MPT} of 5 μl Pd nanoparticles was ~0.261 μg/cm^2 s. The R_{MPT} increases rapidly from ~0.037 μg/cm^2 s for 2 μl Pd nanoparticles to ~0.261 μg/cm^{2}s for 5 μl Pd nanoparticles. The ECD rates determined by theoretical MPT increased rapidly with the amount of Pd nanoparticles.

QCM was conducted to detect in situ the effect of Pd nanoparticles on the actual ECD deposition kinetics and rates. Figure 4 presents the results. Notably, two stages of the ECD deposition kinetics catalyzed by Pd nanoparticles were observed. The typical curve was obtained using 3 μl Pd nanoparticle solution. A short incubation period of ~200 s immediately followed the start of the reaction. The frequency was greatly accelerated in the final deposition stage. In addition, the more on the Pd nanoparticle amount, the less frequency changes on the incubation period proceeded. It was plausibly resulted from the interaction of SDSs which were adsorbed on the particular surface. The information obtained by FE-SEM and EDX further elucidates the ECD mechanisms catalyzed by the prepared Pd nanoparticles. Figures 5, 6, and 7 present FE-SEM images of the surface microstructure formed by 100, 200, and 400 s of ECD on the substrate after the substrate was in each case activated with various amount Pd nanoparticles immersed in an electroless bath. Table 3 presents the results of the elemental analysis by EDX. An ~10.4–13.3 wt% copper and ~26.7–32.9 wt% copper on the plated substrate were deposited in 100 and 200 s, respectively. Hence, the amount of copper increases slowly over the first 200 s of deposition time. It is interesting to note that, however, the sizes of the copper grains whose deposition was catalyzed by Pd nanoparticles in the four cases, were very similar and all below 100 nm, as shown in Figs. 5 and 6. The microstructures formed after 400 s were continuous films with large grains, as presented in Fig. 7. The deposited films were detected to be ~100 wt% copper. Therefore, FE-SEM, EDX, and QCM revealed that ECD growth kinetics can be plausibly divided to two periods. One is the incubation period up to 200 s and the other is the acceleration period after 200 s. In the incubation period, the ECD bath is catalyzed by some Pd nanoparticles and the small copper grains are then slowly deposited. Before the acceleration period, the Pd nanoparticles and small deposited copper grains exhibit high activities on the reducer in the ECD bath, forming continuously conducting films.

Figure 4 fairly compares the activities of the various amounts of Pd nanoparticles, measured by QCM. The deposition rates, R_{QCM}, are calculated from the difference between the electrode frequencies, using Sauerbrey's equation [19]. Table 2 summarizes the results. Notably, the ECD deposition rates increase with the amount of Pd nanoparticles solution, in the order 5>4>3>2 μl. The

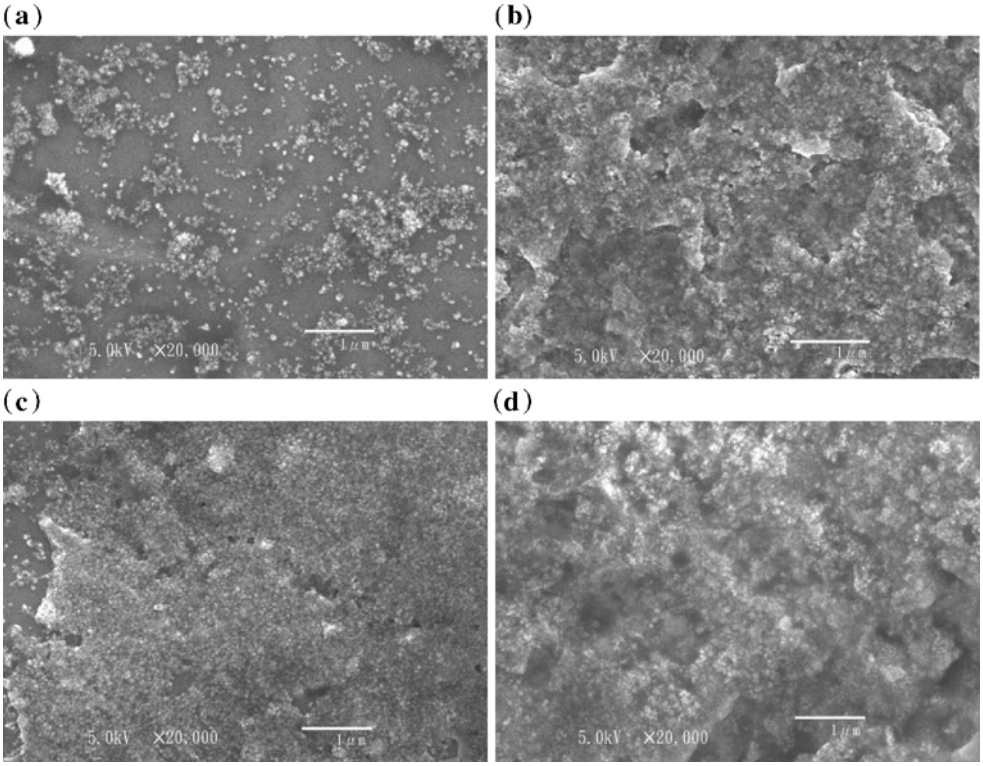

Fig. 5 FE-SEM images of ECD surface microstructure activated by various volumes of Pd nanoparticle solution after a deposition time of 100 s. **a** 2 μl, **b** 3 μl, **c** 4 μl, and **d** 5 μl

R_{QCM} values of 2, 3, 4, and 5 μl of Pd nanoparticles were detected to be approximately ~0.189, ~0.283, ~0.295, and ~0.48 μg/cm^2 s, respectively, revealing that changing the amount of nanocatalyst markedly affects the deposition rate. The trend is consistent with the results obtained using MPT. For a given quantity of catalyst, the actual deposition rate, R_{QCM}, substantially exceeds the MPT value, R_{MPT}, as indicated in Table 2, perhaps because the difference arises from the fact that the cathodic currents that produce hydrogen, in mixed potential theory, are negligible, when

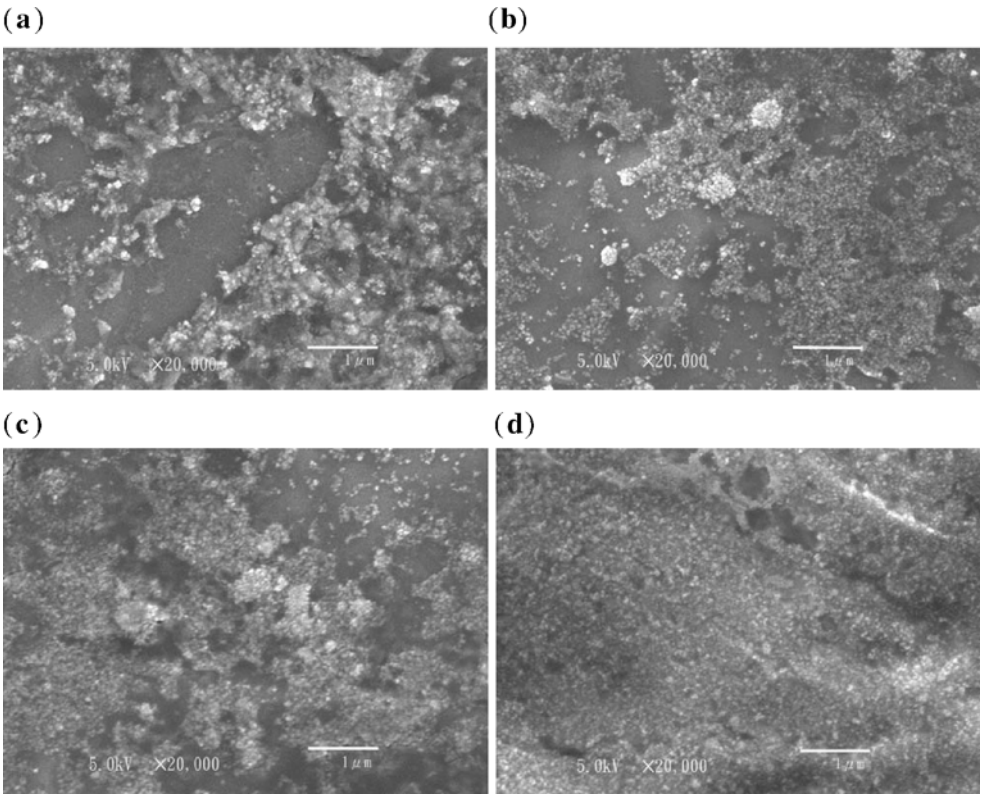

Fig. 6 FE-SEM images of ECD surface microstructure activated by various volumes of Pd nanoparticles solution after a deposition time of 200 s. **a** 2 μl, **b** 3 μl, **c** 4 μl, and **d** 5 μl

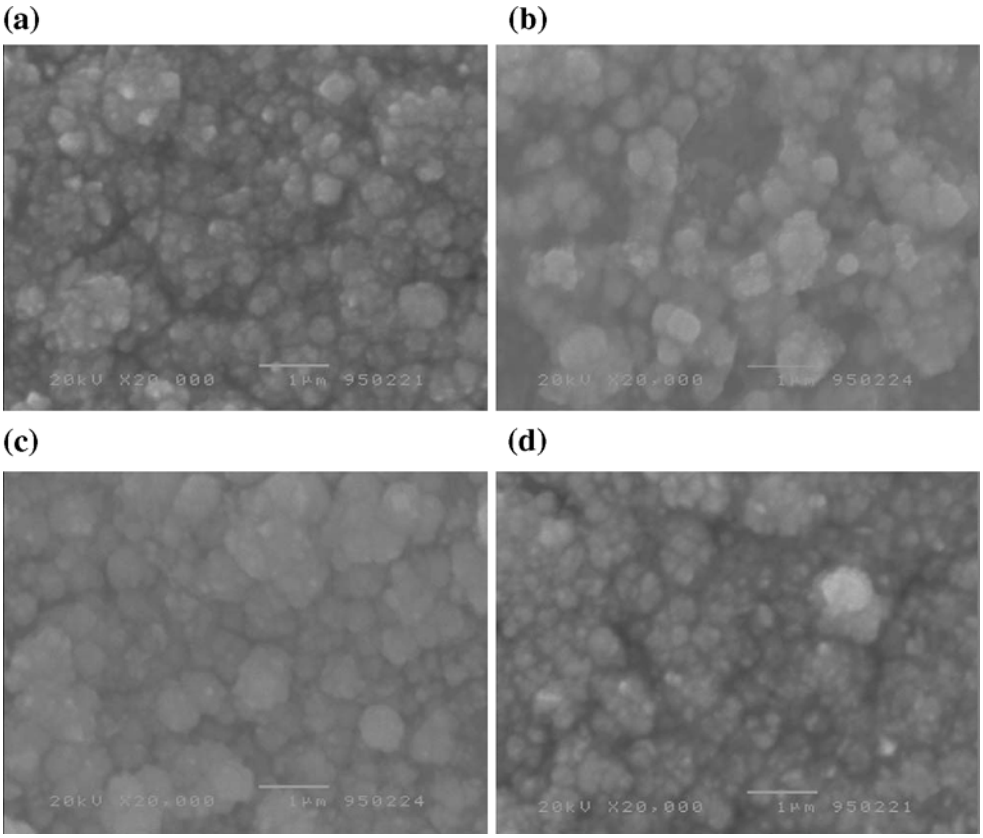

Fig. 7 FE-SEM images of ECD surface microstructure activated by various volumes of Pd nanoparticles solution at a deposition time of 400 s. 2 μl, **b** 3 μl, **c** 4 μl, and **d** 5 μl

the equilibrium potential is reached. Accordingly, the hydrogen-producing reaction strongly affects the ECD kinetics. Notably, the ratio of rates R_{QCM} to R_{MPT} declines as the amount of nanoparticles increases, as presented in Table 2. The theoretical rate determined by mixed potential theory approaches stepwise the true value as the amount of catalyst is used. Increasing the amount of nanocatalyst plausibly increases greatly the intensity of the oxidative and reductive LSV current peaks, corresponding to the deposition rates.

Conclusion

This study investigated the catalytic effect of Pd nanoparticles on the deposition kinetics and the microstructures in (an/the) electroless copper bath. QCM, FE-SEM, and EDX were utilized together to study changes in the ECD kinetics, which occur in two stages—the incubation period and the acceleration period. During the incubation period, small copper particles are deposited. In the acceleration period, the ECD rate increases rapidly and continuously conducting films with large grains are formed. The currents for both oxidation and reduction LSV peaks, corresponding to increasing amounts of Pd nanoparticles, are enhanced. The deposition rate determined by mixed potential theory increased rapidly with the volume of the Pd nanoparticle solution to 5 μl. This trend is consistent with the QCM data, revealing that the quantity of Pd nanoparticles strongly affects the ECD reaction. Based on the findings of this work, the ECD kinetics and mechanism catalyzed by Pd nanoparticles can be further understood in a manner that supports practical applications, such as fabricating electronic nanocircuits in PCB and ULSI.

Table 3 A summary for EDX analysis of ECD layer catalyzed by the Pd nanoparticle solution of the various quantities

	100 s		200 s		400 s	
	Cu (wt%)	Pd (wt%)	Cu (wt%)	Pd (wt%)	Cu (wt%)	Pd (wt%)
2 μl	13.3	86.7	26.7	73.3	99.59	0.41
3 μl	12.1	87.9	29.4	70.6	100	0
4 μl	11.2	88.8	27.6	73.4	100	0
5 μl	10.4	89.6	32.9	67.1	100	0

References

1. Abe S, Ohkubo M, Fujinami T, Honma H (1998) Trans Inst Met Finish 76:12
2. Meyer H, Nichols RJ, Schröer D, Stamp L (1994) Electrochim Acta 39:1325
3. Schacham-Diamand Y, Dubin V, Angyal M (1995) Thin Solid Films 262:93
4. O'Kelly JP, Mongery KF, Gobil Y, Torres J, Kelly PV, Grean GM (2000) Microelectron Eng 50:473
5. Dubin VM, Schacham-Diamand YY (1997) J Electrochem Soc 144:898
6. Shingubara S, Wang Z, Yaegashi O, Obata R, Sakaue H, Takahagi T (2004) Electrochem Solid-State Lett 7:C78
7. Mishra KG, Paramguru RK (1999) Metall Mater Trans B 30b:223
8. Tam TM (1985) J Electrochem Soc 132:806
9. Wanner M, Wies H, Weil KG (1988) Ber Bunsenges Phys Chem 92:736
10. Paunovic MJ (1977) J Electrochem Soc 124:349
11. Jusys Z, Pauliukaité R, Vaškelis A (1999) Phys Chem Chem Phys 1:313
12. Hamilton JF, Baetzold RC (1979) Science 205:1213
13. Mallory GO (1990) The fundamental aspects of electroless nickel plating. In: Mallory GO, Hajdu JB (eds) Electroless plating: fundamentals and applications. American Electroplaters and Surface Finishers Society, Orlando, pp 1–56
14. Sverdlov Y, Bogush V, Einati H, Shacham-Diamand Y (2005) J Electrochem Soc 152:C631
15. Lee CL, Huang YC, Wan CC, Wang YY, Ju YY, Kuo LC, Oung JC (2005) J Electrochem Soc 152:C520
16. Lee CL, Wan CC, Wang YY (2001) Adv Funct Mater 11:344
17. José-Yacamán M, Marín-Almazo M, Ascencio JA (2001) J Mol Catal 173:61
18. Paunovic M, Schlesinger M (1998) Fundamentals of electrochemical deposition. Wiley, New York, pp 133–160
19. Bard AJ, Faulkner LR (2001) Electrochemical methods. Wiley, New York, p 725